

Published in final edited form as:

Nat Cell Biol. 2012 November ; 14(11): 1169–1180. doi:10.1038/ncb2608.

β 2-syntrophin and Par-3 promote an apicobasal Rac activity gradient at cell-cell junctions by differentially regulating Tiam1 activity

Natalie A. Mack¹, Andrew P. Porter¹, Helen J. Whalley¹, Juliane P. Schwarz², Richard C. Jones³, Azharuddin Sajid Syed⁴, Anders Bjartell⁴, Kurt I. Anderson², and Angeliki Malliri¹

¹Cell Signalling Group, Cancer Research UK Paterson Institute for Cancer Research, The University of Manchester, Manchester, M20 4BX, UK

²Tumour Cell Migration Group, Cancer Research UK Beatson Institute for Cancer Research, Glasgow, G61 1BD, UK

³MS Bioworks, 3950 Varsity Drive, Ann Arbor, MI 48108, US

⁴Department of Clinical Sciences, Division of Urological Cancers, Lund University, Skåne University Hospital, Malmö, Sweden

Abstract

Although Rac and its activator Tiam1 are known to stimulate cell-cell adhesion, the mechanisms regulating their activity in cell-cell junction formation are poorly understood. Here, we identify β 2-syntrophin as a Tiam1 interactor required for optimal cell-cell adhesion. We show that during tight junction (TJ) assembly β 2-syntrophin promotes Tiam1-Rac activity, in contrast to the function of the apical determinant Par-3 whose inhibition of Tiam1-Rac activity is necessary for TJ assembly. We further demonstrate that β 2-syntrophin localises more basally than Par-3 at cell-cell junctions, thus generating an apicobasal Rac activity gradient at developing cell-cell junctions. Targeting active Rac to TJs shows that this gradient is required for optimal TJ assembly and apical lumen formation. Consistently, β 2-syntrophin depletion perturbs Tiam1 and Rac localisation at cell-cell junctions and causes defects in apical lumen formation. We conclude that β 2-syntrophin and Par-3 finetune Rac activity along cell-cell junctions controlling TJ assembly and the establishment of apicobasal polarity.

Cell-cell adhesion and apicobasal polarity are critical for epithelial function. In vertebrates, tight junctions (TJs) define the apical–basolateral membrane border^{1,2}, acting as a “gate” by regulating paracellular traffic, and a “fence” by limiting apicobasal diffusion, thereby maintaining apicobasal polarity. Adherens junctions (AJs), located below TJs, provide strong intercellular connections, helping to maintain tissue architecture. Cytoplasmic signalling and scaffolding protein complexes associated with AJs and TJs, such as the Par complex (Par-3-Par-6-atypical Protein Kinase C), regulate junction assembly and polarity³. Disrupted cell-cell adhesion and polarity contributes to tumour development and malignant

AUTHOR CONTRIBUTIONS

N.A.M. performed the majority of the experimental work, data analysis and manuscript preparation. A.P.P. contributed extensively to experiments and preparation of the manuscript. H.J.W. contributed to experiments and analysis. R.C.J. performed the MS analysis. J.P.S. and K.I.A. contributed to and supervised the FLIM-FRET analysis. A.S.S.K. and A.B. performed the TMA staining and scoring together with N.A.M. A.M. was the grant holder and principal investigator who supervised the study and manuscript preparation and made intellectual contributions throughout.

COMPETING FINANCIAL INTERESTS

The authors declare no competing financial interests.

progression⁴⁻⁶. Deciphering the molecular mechanisms regulating cell-cell adhesion and polarity will enhance our understanding of tumourigenesis and potentially improve therapies.

The small GTPase Rac and its activator Tiam1 (T-cell lymphoma invasion and metastasis 1) regulate TJs, AJs, and are implicated in tumourigenesis⁷. However, their exact roles at cell-cell adhesions remain controversial. One study found Tiam1-Rac inhibition to be required for TJ assembly⁸, whilst other studies have shown that Tiam1-Rac activity promotes TJ assembly^{9,10}, consistent with it promoting AJs¹¹⁻¹³. Moreover, precisely how Tiam1 contributes to tumourigenesis remains unknown, although its regulation of cell-cell adhesions, cell cycle progression^{12,14-16} and survival^{14,17-21} are all believed to be important.

To better understand how Tiam1-Rac signalling contributes to tumourigenesis we further investigated its function at cell-cell adhesions. We identified β 2-syntrophin as a Tiam1 interactor and found that in contrast to Par-3⁸, β 2-syntrophin promotes Tiam1-Rac activity during TJ assembly. These differential effects result in an apicobasal Rac activity gradient at developing cell-cell junctions that controls TJ assembly and apicobasal polarity. Finally, we showed that reduced membrane-associated β 2-syntrophin correlates with prostate cancer progression.

RESULTS

A PDZ-mediated interaction between Tiam1 and the β 2-syntrophin-utrophin-dystrobrevin-beta complex

By tandem affinity purification of tagged Tiam1 followed by mass spectrometry, we identified β 2-syntrophin, utrophin and dystrobrevin-beta as Tiam1 interactors among the known interactors 14-3-3, ERK1, Camk2 and Cask^{11,22-24} (Supplementary Information, Table 1). β 2-syntrophin, utrophin and dystrobrevin-beta form a complex localising to the basolateral membrane in MDCKII cells²⁵, however, its role at cell-cell adhesions was unknown. We hypothesised that this complex could be important for Tiam1's function at cell-cell adhesions. We performed co-immunoprecipitations to validate the mass spectrometry results. We found that exogenous Tiam1 co-precipitates endogenous syntrophin and utrophin from HEK293T cells (Fig. 1a). Moreover, endogenous Tiam1 co-precipitated endogenous syntrophin (Fig. 1b), and Tiam1 and β 2-syntrophin co-localised at cell-cell adhesions in MDCKII cells (Fig. 1c). We next defined their interaction domains utilising N-terminally truncated Tiam1-HA constructs and GFP-tagged β 2-syntrophin domain constructs²⁵ (Figs 1d, 1e). We found that the C-terminal 196 amino acids of Tiam1 (C196-Tiam1) and the PDZ domain of β 2-syntrophin were sufficient for the interaction (Fig. 1f and Supplementary Information, S1a, S1b). C196-Tiam1 contains the internal sequence KETDI matching the consensus syntrophin PDZ-binding motif (PBM), K/R-E-(S/T)-X-(V/L/I/M)²⁶ (Fig. 1d and Supplementary Information, Fig. S1c). Deletion of KETDI from C196-Tiam1 (Fig. 1f), and from full-length Tiam1 (Fig. 1g), abolished the interaction with β 2-syntrophin, despite there being additional sequences in Tiam1 matching the consensus syntrophin PBM (Supplementary Information, Fig. S1c). Two short Tiam1 fragments containing KETDI (KETDI-19 and KETDI-27) did not bind or bound only weakly to β 2-syntrophin, whereas a longer fragment (KETDI-44) did interact (Fig. 1h and Supplementary Information, Fig. S1d), suggesting the interaction requires residues flanking KETDI. Furthermore, KETDI was required for the Tiam1-utrophin interaction (Fig. 1g) and β 2-syntrophin knockdown abolished the Tiam1-utrophin interaction (Fig. 1i), suggesting that Tiam1 interacts with utrophin indirectly via β 2-syntrophin. The KETDI sequence is highly conserved in Tiam1 orthologues (Supplementary Information, Fig. S1e), indicating the importance of the interaction for Tiam1 function. Notably, this sequence is found in Tiam2 (Stef) (Supplementary Information, Fig. S1e).

β 2-syntrophin regulates TJ assembly

We next investigated whether β 2-syntrophin regulates cell-cell adhesion similarly to Tiam1⁸⁻¹³. For this we engineered MDCKII cells with doxycycline-inducible expression of shRNA sequences targeting *β 2-syntrophin* and a non-targeting control (Figs 2a, 2b). Calcium withdrawal disassembles cell-cell adhesions which is reversed by calcium readdition²⁷ (calcium switch, CS). The remodelling of junctional complexes following CS mimics events accompanying epithelial cell movements during wound closure and tumour development. TJ integrity can be assessed by measuring transepithelial electrical resistance (TER) of cell monolayers grown on transwell filters and together with immunostaining for TJ markers has been widely used to identify TJ assembly regulators^{8,10,28,29}. We found that β 2-syntrophin knockdown in MDCKII cells markedly retards CS-induced TER development, indicating defective TJ assembly (Fig. 2c). We confirmed the TER defect was β 2-syntrophin-dependent by rescuing with expression of shRNA-resistant β 2-syntrophin (Figs 2d, 2e). Immunofluorescence for the TJ marker occludin after CS confirmed a delay in TJ assembly (Fig. 2f). We also observed delayed TJ assembly after plating (Figs 2g, 2h), confirming the defects are not CS-specific. Immunostaining for β -catenin revealed impaired AJ assembly in β 2-syntrophin knockdown cells (Supplementary Information, Fig. S2a). It is possible that the TJ assembly defects result from defective AJ formation. By performing hanging-drop assays to assess the aggregation ability of single cells, we also found that β 2-syntrophin knockdown impedes cell-cell aggregation (Supplementary Information, Figs S2b, S2c). Moreover, a cell-dissociation assay demonstrated that β 2-syntrophin knockdown compromises cell-cell adhesion strength (Supplementary Information, Fig. S2d). Together, these results demonstrate that β 2-syntrophin regulates epithelial cell-cell adhesions.

Tiam1-induced Rac activity impedes TJ assembly

To relate β 2-syntrophin function at cell-cell adhesions to its Tiam1 interaction, we further interrogated Tiam1 function in TJ assembly, since previous studies are conflicting⁸⁻¹⁰. We found that doxycycline-inducible Tiam1 knockdown in MDCKII cells for either a short or long period did not inhibit CS-induced TER development, but slightly enhanced it (Figs 3a-d). Tiam1 knockdown with an alternative shRNA did not alter TER, likely due to less-efficient knockdown (Supplementary Information, Figs S3a-d). We next found that Tiam1-HA-WT over-expression retarded CS-induced TER development (Fig. 3e). Immunostaining for occludin (Fig. 3f) and quantifying the number of intact junctions (Fig. 3g) confirmed delayed TJ assembly. To investigate whether this was through Rac activation, we analysed the effect of over-expressing dominant-negative/GEF-dead Tiam1 (Tiam1-HA-DH*) at levels comparable to Tiam1-HA-WT (Supplementary Information, Fig. S3e). Tiam1-HA-DH* expression enhanced CS-induced TER development (Fig. 3h) consistent with our Tiam1 knockdown data. Immunostaining for occludin at 15 min following CS (Fig. 3i) and quantifying the number of intact junctions (Fig. 3j) confirmed accelerated TJ assembly. Collectively, these results show that Tiam1-induced Rac activity impedes TJ assembly in MDCKII cells, consistent with the findings of Chen and Macara⁸.

β 2-syntrophin promotes Tiam1-Rac activity during TJ assembly

We next investigated whether the ability of over-expressed Tiam1 to inhibit TJ assembly requires its interaction with β 2-syntrophin. Expression of Tiam1-HA- Δ KETDI at levels comparable to Tiam1-HA-WT (Supplementary Information, Fig. S4a) had little effect on CS-induced TER development (Fig. 4a). Likewise, no significant change in TJ assembly was observed following immunostaining for occludin (Fig. 4b) and quantification of intact junctions (Fig. 4c). Since the inhibition of TJ assembly by over-expressed Tiam1 requires its Rac-GEF activity (Figs 3h-j), we hypothesised that β 2-syntrophin promotes Tiam1-mediated Rac activation during TJ assembly. We therefore compared Rac activity levels in cells expressing Tiam1-HA-WT, Δ KETDI or Δ DH* either maintained in high calcium medium

(HCM) or at 60 min following CS. In parental and Tiam1-HA-WT expressing MDCKII cells Rac activity at 60 min following CS is induced to levels similar to HCM (Supplementary Information, Fig. S4b, and Fig. 4d). In contrast, Tiam1-HA- Δ KETDI expressing cells showed reduced Rac activity at 60 min following CS (Fig. 4d), which was significantly lower than in Tiam1-HA-WT expressing cells (Fig. 4e). Cells expressing Tiam1-HA-DH* had low Rac activity under both HCM and CS conditions (Fig. 4d).

We next investigated whether β 2-syntrophin knockdown affects Rac activity. Control and β 2-syntrophin knockdown cells had comparable levels of Rac activity in HCM (Figs 4f, 4g). However, β 2-syntrophin knockdown cells had reduced CS-induced Rac activation (Figs 4h, 4i), consistent with reduced Tiam1 activity since Tiam1 is also required for CS-induced Rac activation (Figs 4j, 4k). Importantly, β 2-syntrophin knockdown did not increase the endogenous Tiam1-Par-3 interaction at 60 min following CS (Supplementary Information, Figs S4c, S4d), excluding the possibility that the Rac activation defects are due to an increase in the inhibitory Par-3-Tiam1 interaction⁸.

We next analysed the effect of inhibiting the Tiam1- β 2-syntrophin interaction on CS-induced Rac activation. Expression of the Tiam1 fragment KETDI-44 reduced the endogenous interaction (Fig. 4l). Inducible KETDI-44 expression inhibited CS-induced Rac activation (Figs 4m, 4n), providing further evidence that β 2-syntrophin promotes CS-induced Rac activation through binding Tiam1. Furthermore, we observed β 2-syntrophin, along with E-cadherin and Par-3, localising to cell-cell junctions at 60 min after CS (Supplementary Information, Fig. S4e). Together, these results suggest that β 2-syntrophin promotes Tiam1-Rac activity at developing cell-cell junctions in MDCKII cells.

β 2-syntrophin and Par-3 localise differently along the apicobasal axis

Initially it seemed counterintuitive that β 2-syntrophin, an apparent positive regulator of TJ assembly, would promote Tiam1-Rac activity, an apparent negative regulator of TJ assembly. However, the contribution of Tiam1 to CS-induced Rac activation (Figs 4j, 4k), indicates also a positive role during TJ assembly. To rationalise our data, and considering the inhibitory effect of Par-3 on Tiam1 during TJ assembly⁸, we postulated that both inhibitors and activators of Tiam1-Rac control TJ assembly. We hypothesised that β 2-syntrophin and Par-3 localise differently at cell-cell junctions, thereby spatially regulating Tiam1-Rac activity, which might in turn drive optimal TJ assembly. To investigate this, we analysed Par-3, β 2-syntrophin and Tiam1 localisations along the apicobasal axis of MDCKII cells. We found that β 2-syntrophin localises more basally than Par-3, although with some overlap (Figs 5a, 5b). Quantifying staining intensities at individual junctions confirmed the differential localisations of Par-3 and β 2-syntrophin (Figs. 5c, 5d), and revealed that while Tiam1 and Par-3 overlap, the peak of Tiam1 expression was below that of Par-3 (Fig. 5c). In β 2-syntrophin knockdown cells, while both Tiam1 and Par-3 still localised to cell-cell junctions, we observed a significant shift in Tiam1 localisation in the apical direction relative to Par-3 (Figs 5e-g). It is possible that β 2-syntrophin promotes TJ assembly through maintaining correct Tiam1 localisation along the apicobasal axis, in addition to regulating Tiam1 activity.

Staining for the AJ marker E-cadherin revealed that both β 2-syntrophin and Tiam1 are present at AJs with low levels of Par-3 (Figs 5h, 5i and Supplementary Information, S5a, S5b). Staining for occludin revealed that Par-3, as anticipated, is mainly present at TJs (Supplementary Information, Figs S5c, S5d). These stainings imply the presence of a Par-3-Tiam1 complex at TJs and a separate β 2-syntrophin-Tiam1 complex at AJs. Consistent with this, β 2-syntrophin over-expression reduced the Tiam1-Par-3 interaction (Figs 5j, 5k), indicative of competition between the two complexes and supporting our conclusion that Tiam1 is regulated by different complexes at distinct cell-cell junction locations. From our

immunostaining results, we cannot exclude the possibility of a ternary Tiam1-Par-3- β 2-syntrophin complex, although the lack of a detectable Par-3- β 2-syntrophin interaction (Supplementary Information, S5e) suggests any such complex is transitory or contains only a small proportion of the available proteins.

A Rac activity gradient exists along the apicobasal axis

We next investigated whether there is a gradient of Rac localisation and/or activity along the apicobasal axis of developing cell-cell junctions. Immunostaining for endogenous Rac and Par-3 after CS revealed that Rac is localised more basally than Par-3 at cell-cell junctions (Figs 6a, 6b). We verified the Rac antibody for immunostaining using Rac1 knockdown and GFP-Rac1 over-expression (Supplementary Information, Figs S6a-c). Quantification of staining intensities at individual junctions confirmed the differential localisations of Par-3 and Rac (Figs. 6c, 6d). These results suggested that Rac activity is spatially regulated along the apicobasal axis of cell-cell junctions. To address this directly, we performed FLIM-FRET (fluorescence lifetime imaging microscopy-fluorescence resonance energy transfer) analysis of a Rac biosensor in live MDCKII cells as done previously for Rho³⁰. We generated MDCKII cells expressing a membrane-targeted RFP-GFP variant of the Raichu-Rac FRET reporter³¹ and confirmed reporter function by performing FLIM-FRET analysis before and after treatment with hepatocyte growth factor (HGF), a known stimulator of Rac activity (Supplementary Information, Fig. S6d). Next, we performed FLIM-FRET analysis after CS in cells expressing either Raichu-Rac or membrane-targeted GFP control. We measured average fluorescence lifetimes across individual cell-cell junctions at 0.5 μ m steps along the z-axis and compared average lifetimes at apical junctional positions (TJs) with those 1 μ m below (subapical junctions). We observed no significant lifetime changes in control GFP cells (Supplementary Information, Figs S6e, S6f). Notably, we observed significantly reduced fluorescence lifetimes of Raichu-Rac, and therefore increased Rac activity, at subapical junctions compared to apical junctions (Supplementary Information, Figs S6g, S6h). These data confirmed that changes in Rac staining intensity correlate with changes in Rac activity.

Our data demonstrate the existence of an apicobasal Rac activity gradient at cell-cell junctions and we propose that β 2-syntrophin and Par-3 are important determinants through their differential regulation of Tiam1 activity. To directly show that β 2-syntrophin contributes to the gradient, we analysed Rac localisation after CS in β 2-syntrophin knockdown cells. Rac was less separated from Par-3 in β 2-syntrophin knockdown cells (Figs 6e, 6f) compared with controls (Figs 6a-d). Quantification revealed a significant shift of Rac in the apical direction relative to Par-3 (Fig. 6g) possibly as a consequence of shifted Tiam1 (Fig. 5g). We next performed FLIM-FRET analysis after CS in non-targeting RNAi and β 2-syntrophin knockdown Raichu-Rac expressing MDCKII cells (Supplementary Information, Fig. S6i). We observed significantly reduced fluorescence lifetimes at subapical junctions compared to apical junctions in non-targeting RNAi cells (Figs 6h, 6i), consistent with the results above (Supplementary Information, Figs S6g, S6h), while we found no significant lifetime changes in β 2-syntrophin knockdown cells (Figs 6h, 6i). These results together with our immunostaining data show that the Rac gradient is diminished in β 2-syntrophin knockdown cells.

We next investigated the effect of Tiam1 knockdown on the Rac activity gradient using FLIM-FRET analysis. We found significantly reduced fluorescence lifetimes at subapical compared to apical junctions in Tiam1 knockdown cells, similarly to controls (Supplementary Information, Figs S6i-k). This indicates a Rac activity gradient can still be formed in Tiam1 knockdown cells, consistent with their ability to form TJs (Figs 3a, 3c). However, we cannot rule out changes to the steepness of the Rac gradient in Tiam1 knockdown cells, which may account for their slightly enhanced CS-induced TER

development (Figs 3a, 3c). In these cells, compensatory mechanisms may exist to differentially regulate apicobasal Rac activity. Alternatively, residual Tiam1 may be sufficient to generate a gradient of Rac activity.

Spatial regulation of Rac activity is important for TJ assembly and polarity

To assess the importance of the Rac activity gradient for TJ assembly, we analysed the effect of targeting constitutively active Rac1 (Rac1-V12) to TJs on CS-induced TER development. We used the GBP (GFP-binding protein) targeting system³²⁻³⁵ to force an interaction between occludin and Rac1-V12 (Fig. 7a). We confirmed that GBP-tagged occludin and GFP-tagged Rac1-V12 co-expressed in MDCKII cells interact (Supplementary Information, Fig. S7a), resulting in their co-localisation at cell-cell junctions (Fig. 7b). MDCKII cells expressing GBP-occludin alone, GFP-Rac1-V12 alone, or GBP-occludin with either GFP, GFP-Rac1-V12, or GFP-Rac1-WT were generated. GFP-Rac1-V12 and GFP-Rac1-WT were expressed at levels lower than endogenous Rac (Supplementary Information, Figs S7b, S7c) to minimise adverse effects of over-expression. While targeting Rac1-V12 to TJs was anticipated to disrupt the Rac activity gradient, Rac1-WT was expected to be less disruptive due to low abundance of Rac activators apically. Cells expressing GBP-occludin with GFP-Rac1-V12 had reduced CS-induced TER development indicating TJ assembly defects compared to all controls, including cells expressing GBP-occludin with GFP-Rac1-WT (Fig. 7c).

Since TJ assembly and apical lumen formation are tightly connected^{8,36-38}, we hypothesised that disrupting the Rac activity gradient may perturb apical lumen formation. Cells expressing GBP-occludin with GFP-Rac1-V12 produced more multi-lumen cysts compared with controls when grown in collagen I matrix (Figs 7d, 7e), indicative of impaired apicobasal polarity³⁹. Expression of Rac1-V12 alone did not affect cyst development (Supplementary Information, Figs S7d, S7e). These results suggest that the apicobasal Rac activity gradient at cell-cell junctions regulates TJ assembly and the establishment of apicobasal polarity.

β 2-syntrophin regulates polarity and is a potential tumour suppressor in the human prostate

The above results suggest that deregulation of the Rac activity gradient can disrupt TJ integrity and apicobasal polarity, potentially promoting cell proliferation and tumour formation^{2,4,7,40-42}. Therefore, we predicted that β 2-syntrophin loss from cell-cell adhesions would disrupt apicobasal polarity and promote tumorigenesis. To address this, we first investigated whether β 2-syntrophin regulates apical lumen formation. β 2-syntrophin knockdown cells produced mostly multi-lumen cysts (Figs 8a, 8b and Supplementary Information, Fig. S8a), consistent with our results with Rac1-V12 targeted to TJs (Figs 7d, 7e).

Membrane-localised β 2-syntrophin has been documented in normal prostate tissue (URL:<http://www.proteinatlas.org/ENSG00000168807/normal>). Moreover, Tiam1 over-expression correlates with poor prognosis of human prostate cancer⁴³. Additionally, Rac expression has been observed in healthy prostate tissue and increased Rac expression correlates with prostate cancer progression^{44,45}. We therefore hypothesised that the β 2-syntrophin-Tiam1-Rac signalling pathway may be deregulated in human prostate cancer. We stained a prostate cancer tissue microarray (TMA) with an anti- β 2-syntrophin antibody and scored its expression levels in both malignant and pre-malignant areas (Supplementary Information, Table 2). β 2-syntrophin expression was frequently reduced in malignant compared with pre-malignant areas within the same tumour section (Supplementary Information, Figs S8b, S8c and Tables 2, 3). However, no significant correlation was found

between malignant expression and Primary Gleason scores (Supplementary Information, Fig. S8d), indicating that β 2-syntrophin down-regulation is an early event in prostate cancer pathogenesis.

Subsequently, we scored subcellular localisation of β 2-syntrophin in malignant areas. Membrane β 2-syntrophin intensity scores were obtained by combining the expression and localisation scores (Supplementary Information, Table 2). We found a significant negative correlation between membrane β 2-syntrophin intensity and Primary Gleason score (Supplementary Information, Fig. S8e), revealing that β 2-syntrophin is frequently lost from cell-cell adhesions during prostate cancer progression (Supplementary Information, Fig. S8f). Performing classification regression tree analyses⁴⁶ to divide the membrane intensity scores into weak and strong subgroups revealed a significant association between membrane β 2-syntrophin intensity and BCR (time to biochemical recurrence) free time (Supplementary Information, Fig. S8g), indicating that patients showing reduced β 2-syntrophin levels at cell-cell adhesions are more likely to relapse.

DISCUSSION

We have shown that β 2-syntrophin, and associated utrophin-dystrobrevin-beta, interact with an internal PBM on Tiam1— a rare mode of PDZ recognition⁴⁷⁻⁵². We infer that the differential effects of β 2-syntrophin and Par-3 on Tiam1-Rac activity, in conjunction with their differential but also overlapping localisations, enable them to promote an apicobasal Rac activity gradient at cell-cell junctions (see models; Figs 8c, 8d), which is required for optimal establishment of TJs and apicobasal polarity.

Our findings support those of Georgiou et al. whose data implied that differential apicobasal Rac activity exists in *Drosophila* columnar epithelia⁵³. Here, we have directly visualised an apicobasal Rac activity gradient in mammalian epithelial cells and relate it to TJ formation and apical lumen formation. Our results also have parallels with those of Yagi et al. which demonstrated low apical Rac activity in MDCKII cysts⁵⁴. The β 2-syntrophin-Tiam1-Rac pathway might also regulate apicobasal polarity by alternative means: Tiam1, Rac, and the Dystroglycan-Par-1b complex of which syntrophin is a part all regulate laminin deposition which is important for apicobasal polarity^{55,56,57}.

Our data enhances our understanding of tumourigenesis. We propose that deregulation of β 2-syntrophin, Par-3, or Tiam1, would disrupt the Rac activity gradient, and in turn disrupt TJs and apicobasal polarity, promoting tumourigenesis^{2,4,7,40-42}. In agreement is our finding that increased Tiam1-Rac activity impedes TJ assembly and the findings of Yagi et al. showing that Tiam1 over-expression at the entire plasma membrane disrupts apicobasal polarity⁵⁴. Moreover, Tiam1 over-expression occurs in many human tumours^{43,58-63} and correlates with prostate cancer progression³⁹. Our TMA data suggests that reduced membrane-associated β 2-syntrophin is another mechanism by which Tiam1-Rac signalling at cell-cell junctions is deregulated and highlights the potential of β 2-syntrophin as a biomarker for prostate cancer progression and prognosis. Loss of function mutations reported for utrophin could be another mechanism⁶⁴.

The coordinated action of multiple protein complexes is a well-established mechanism of regulation of cell-cell adhesion and polarity⁶⁵. Our data show that cooperation between the Tiam1- β 2-syntrophin-utrophin-dystrobrevin-beta and Tiam1-Par-3 complexes generates finely-tuned spatial distribution of Rac activity at cell-cell junctions, controlling TJ formation and apicobasal polarity. This may explain previously reported cell-cell adhesion defects following either global Rac activation or inhibition (see our review⁷).

Supplementary Material

Refer to Web version on PubMed Central for supplementary material.

Acknowledgments

This work was supported by Cancer Research UK grant number C147/A6058 and Medical Research Council grant number MR/J00104X/1. We thank colleagues mentioned in the Methods for providing reagents; E. Nilsson for immunohistochemical stainings; S. Bagley and A. Dunne for help with microscopy and image analysis; C. O'Neill, M. Balda, S. Ohno, and V. Braga for technical advice; A. Hurlstone, I. Hagan, D. Garrod, J. Brognard and members of the Cell Signalling Group for helpful discussions and critical reading of the manuscript.

References

1. Matter K, Aijaz S, Tsapara A, Balda MS. Mammalian tight junctions in the regulation of epithelial differentiation and proliferation. *Curr Opin Cell Biol.* 2005; 17:453–8. [PubMed: 16098725]
2. Steed E, Balda MS, Matter K. Dynamics and functions of tight junctions. *Trends Cell Biol.* 2010; 20:142–9. [PubMed: 20061152]
3. Assemat E, Bazellieres E, Pallesi-Pocachard E, Le Bivic A, Massey-Harroche D. Polarity complex proteins. *Biochim Biophys Acta.* 2008; 1778:614–30. [PubMed: 18005931]
4. Feigin ME, Muthuswamy SK. Polarity proteins regulate mammalian cell-cell junctions and cancer pathogenesis. *Curr Opin Cell Biol.* 2009; 21:694–700. [PubMed: 19729289]
5. McCaffrey LM, Macara IG. Epithelial organization, cell polarity and tumorigenesis. *Trends Cell Biol.* 2011; 21:727–35. [PubMed: 21782440]
6. Royer C, Lu X. Epithelial cell polarity: a major gatekeeper against cancer? *Cell Death Differ.* 2011; 18:1470–7. [PubMed: 21617693]
7. Mack NA, Whalley HJ, Castillo-Lluva S, Malliri A. The diverse roles of Rac signaling in tumorigenesis. *Cell Cycle.* 2011; 10:1571–81. [PubMed: 21478669]
8. Chen X, Macara IG. Par-3 controls tight junction assembly through the Rac exchange factor Tiam1. *Nat Cell Biol.* 2005; 7:262–9. [PubMed: 15723052]
9. Mertens AE, Rygiel TP, Olivo C, van der Kammen R, Collard JG. The Rac activator Tiam1 controls tight junction biogenesis in keratinocytes through binding to and activation of the Par polarity complex. *J Cell Biol.* 2005; 170:1029–37. [PubMed: 16186252]
10. Guillemot L, Paschoud S, Jond L, Foglia A, Citi S. Paracingulin regulates the activity of Rac1 and RhoA GTPases by recruiting Tiam1 and GEF-H1 to epithelial junctions. *Mol Biol Cell.* 2008; 19:4442–53. [PubMed: 18653465]
11. Woodcock SA, et al. SRC-induced disassembly of adherens junctions requires localized phosphorylation and degradation of the rac activator tiam1. *Mol Cell.* 2009; 33:639–53. [PubMed: 19285946]
12. Malliri A, van Es S, Huveneers S, Collard JG. The Rac exchange factor Tiam1 is required for the establishment and maintenance of cadherin-based adhesions. *J Biol Chem.* 2004; 279:30092–8. [PubMed: 15138270]
13. Hordijk PL, et al. Inhibition of invasion of epithelial cells by Tiam1-Rac signaling. *Science.* 1997; 278:1464–6. [PubMed: 9367959]
14. Malliri A, et al. Mice deficient in the Rac activator Tiam1 are resistant to Ras-induced skin tumours. *Nature.* 2002; 417:867–71. [PubMed: 12075356]
15. Malliri A, et al. The rac activator Tiam1 is a Wnt-responsive gene that modifies intestinal tumor development. *J Biol Chem.* 2006; 281:543–8. [PubMed: 16249175]
16. Woodcock SA, et al. Tiam1-Rac signaling counteracts Eg5 during bipolar spindle assembly to facilitate chromosome congression. *Curr Biol.* 2010; 20:669–75. [PubMed: 20346677]
17. Otsuki Y, et al. Guanine nucleotide exchange factor, Tiam1, directly binds to c-Myc and interferes with c-Myc-mediated apoptosis in rat-1 fibroblasts. *J Biol Chem.* 2003; 278:5132–40. [PubMed: 12446731]

18. Rygiel TP, Mertens AE, Strumane K, van der Kammen R, Collard JG. The Rac activator Tiam1 prevents keratinocyte apoptosis by controlling ROS-mediated ERK phosphorylation. *J Cell Sci.* 2008; 121:1183–92. [PubMed: 18349077]
19. Qi H, et al. Caspase-mediated cleavage of the TIAM1 guanine nucleotide exchange factor during apoptosis. *Cell Growth Differ.* 2001; 12:603–11. [PubMed: 11751455]
20. Minard ME, Ellis LM, Gallick GE. Tiam1 regulates cell adhesion, migration and apoptosis in colon tumor cells. *Clin Exp Metastasis.* 2006; 23:301–13. [PubMed: 17086355]
21. Joneson T, Bar-Sagi D. Suppression of Ras-induced apoptosis by the Rac GTPase. *Mol Cell Biol.* 1999; 19:5892–901. [PubMed: 10454536]
22. Woodcock SA, Jones RC, Edmondson RD, Malliri A. A modified tandem affinity purification technique identifies that 14-3-3 proteins interact with Tiam1, an interaction which controls Tiam1 stability. *J Proteome Res.* 2009; 8:5629–41. [PubMed: 19899799]
23. Fleming IN, Elliott CM, Buchanan FG, Downes CP, Exton JH. Ca²⁺/calmodulin-dependent protein kinase II regulates Tiam1 by reversible protein phosphorylation. *J Biol Chem.* 1999; 274:12753–8. [PubMed: 10212259]
24. Stafford RL, Ear J, Knight MJ, Bowie JU. The molecular basis of the Caskin1 and Mint1 interaction with CASK. *J Mol Biol.* 2011; 412:3–13. [PubMed: 21763699]
25. Kachinsky AM, Froehner SC, Milgram SL. A PDZ-containing scaffold related to the dystrophin complex at the basolateral membrane of epithelial cells. *J Cell Biol.* 1999; 145:391–402. [PubMed: 10209032]
26. Gee SH, et al. Cyclic peptides as non-carboxyl-terminal ligands of syntrophin PDZ domains. *J Biol Chem.* 1998; 273:21980–7. [PubMed: 9705339]
27. Noren NK, Niessen CM, Gumbiner BM, Burridge K. Cadherin engagement regulates Rho family GTPases. *J Biol Chem.* 2001; 276:33305–8. [PubMed: 11457821]
28. McNeil E, Capaldo CT, Macara IG. Zonula occludens-1 function in the assembly of tight junctions in Madin-Darby canine kidney epithelial cells. *Mol Biol Cell.* 2006; 17:1922–32. [PubMed: 16436508]
29. Zheng B, Cantley LC. Regulation of epithelial tight junction assembly and disassembly by AMP-activated protein kinase. *Proc Natl Acad Sci U S A.* 2007; 104:819–22. [PubMed: 17204563]
30. Timpson P, et al. Spatial regulation of RhoA activity during pancreatic cancer cell invasion driven by mutant p53. *Cancer Res.* 2011; 71:747–57. [PubMed: 21266354]
31. Yoshizaki H, et al. Activity of Rho-family GTPases during cell division as visualized with FRET-based probes. *J Cell Biol.* 2003; 162:223–32. [PubMed: 12860967]
32. Bertazzi DT, Kurtulmus B, Pereira G. The cortical protein Lte1 promotes mitotic exit by inhibiting the spindle position checkpoint kinase Kin4. *J Cell Biol.* 2011; 193:1033–48. [PubMed: 21670215]
33. Rothbauer U, et al. Targeting and tracing antigens in live cells with fluorescent nanobodies. *Nat Methods.* 2006; 3:887–9. [PubMed: 17060912]
34. Rothbauer U, et al. A versatile nanotrapp for biochemical and functional studies with fluorescent fusion proteins. *Mol Cell Proteomics.* 2008; 7:282–9. [PubMed: 17951627]
35. Schornack S, et al. Protein mislocalization in plant cells using a GFP-binding chromobody. *Plant J.* 2009; 60:744–54. [PubMed: 19686537]
36. Ferrari A, Veligodskiy A, Berge U, Lucas MS, Kroschewski R. ROCK-mediated contractility, tight junctions and channels contribute to the conversion of a preapical patch into apical surface during isochoric lumen initiation. *J Cell Sci.* 2008; 121:3649–63. [PubMed: 18946028]
37. Delous M, et al. Nephrocystin-1 and nephrocystin-4 are required for epithelial morphogenesis and associate with PALS1/PATJ and Par6. *Hum Mol Genet.* 2009; 18:4711–23. [PubMed: 19755384]
38. Horikoshi Y, et al. Interaction between PAR-3 and the aPKC-PAR-6 complex is indispensable for apical domain development of epithelial cells. *J Cell Sci.* 2009; 122:1595–606. [PubMed: 19401335]
39. Schluter MA, Margolis B. Apical lumen formation in renal epithelia. *J Am Soc Nephrol.* 2009; 20:1444–52. [PubMed: 19497970]

40. Miyoshi J, Takai Y. Molecular perspective on tight-junction assembly and epithelial polarity. *Adv Drug Deliv Rev.* 2005; 57:815–55. [PubMed: 15820555]
41. Balda MS, Matter K. Tight junctions and the regulation of gene expression. *Biochim Biophys Acta.* 2009; 1788:761–7. [PubMed: 19121284]
42. Brennan K, Offiah G, McSherry EA, Hopkins AM. Tight junctions: a barrier to the initiation and progression of breast cancer? *J Biomed Biotechnol.* 2010; 2010:460607. [PubMed: 19920867]
43. Engers R, et al. Prognostic relevance of Tiam1 protein expression in prostate carcinomas. *Br J Cancer.* 2006; 95:1081–6. [PubMed: 17003780]
44. Kobayashi T, et al. Activation of Rac1 is closely related to androgen-independent cell proliferation of prostate cancer cells both in vitro and in vivo. *Mol Endocrinol.* 2010; 24:722–34. [PubMed: 20203103]
45. Engers R, et al. Prognostic relevance of increased Rac GTPase expression in prostate carcinomas. *Endocr Relat Cancer.* 2007; 14:245–56. [PubMed: 17639041]
46. Dahlman A, et al. Evaluation of the prognostic significance of MSMB and CRISP3 in prostate cancer using automated image analysis. *Mod Pathol.* 2011; 24:708–19. [PubMed: 21240253]
47. Hillier BJ, Christopherson KS, Prehoda KE, Brecht DS, Lim WA. Unexpected modes of PDZ domain scaffolding revealed by structure of nNOS-syntrophin complex. *Science.* 1999; 284:812–5. [PubMed: 10221915]
48. Harris BZ, Hillier BJ, Lim WA. Energetic determinants of internal motif recognition by PDZ domains. *Biochemistry.* 2001; 40:5921–30. [PubMed: 11352727]
49. Penkert RR, DiVittorio HM, Prehoda KE. Internal recognition through PDZ domain plasticity in the Par-6-Pals1 complex. *Nat Struct Mol Biol.* 2004; 11:1122–7. [PubMed: 15475968]
50. Wong HC, et al. Direct binding of the PDZ domain of Dishevelled to a conserved internal sequence in the C-terminal region of Frizzled. *Mol Cell.* 2003; 12:1251–60. [PubMed: 14636582]
51. London TB, Lee HJ, Shao Y, Zheng J. Interaction between the internal motif KTXXXI of Idax and mDvl PDZ domain. *Biochem Biophys Res Commun.* 2004; 322:326–32. [PubMed: 15313210]
52. Lemaire JF, McPherson PS. Binding of Vac14 to neuronal nitric oxide synthase: Characterisation of a new internal PDZ-recognition motif. *FEBS Lett.* 2006; 580:6948–54. [PubMed: 17161399]
53. Georgiou M, Baum B. Polarity proteins and Rho GTPases cooperate to spatially organise epithelial actin-based protrusions. *J Cell Sci.* 2010; 123:1089–98. [PubMed: 20197404]
54. Yagi S, Matsuda M, Kiyokawa E. Suppression of Rac1 activity at the apical membrane of MDCK cells is essential for cyst structure maintenance. *EMBO Rep.* 2012
55. Masuda-Hirata M, et al. Intracellular polarity protein PAR-1 regulates extracellular laminin assembly by regulating the dystroglycan complex. *Genes Cells.* 2009; 14:835–50. [PubMed: 19549170]
56. O'Brien LE, et al. Rac1 orientates epithelial apical polarity through effects on basolateral laminin assembly. *Nat Cell Biol.* 2001; 3:831–8. [PubMed: 11533663]
57. Hamelers IH, et al. The Rac activator Tiam1 is required for (alpha)3(beta)1-mediated laminin-5 deposition, cell spreading, and cell migration. *J Cell Biol.* 2005; 171:871–81. [PubMed: 16330714]
58. Lane J, Martin TA, Mansel RE, Jiang WG. The expression and prognostic value of the guanine nucleotide exchange factors (GEFs) Trio, Vav1 and TIAM-1 in human breast cancer. *Int Semin Surg Oncol.* 2008; 5:23. [PubMed: 18925966]
59. Yang W, et al. Up-regulation of Tiam1 and Rac1 Correlates with Poor Prognosis in Hepatocellular Carcinoma. *Jpn J Clin Oncol.* 2010
60. Ding Y, et al. Overexpression of Tiam1 in hepatocellular carcinomas predicts poor prognosis of HCC patients. *Int J Cancer.* 2009; 124:653–8. [PubMed: 18972435]
61. Qi Y, et al. Prognostic value of Tiam1 and Rac1 overexpression in nasopharyngeal carcinoma. *ORL J Otorhinolaryngol Relat Spec.* 2009; 71:163–71. [PubMed: 19506399]
62. Liu L, Wu DH, Ding YQ. Tiam1 gene expression and its significance in colorectal carcinoma. *World J Gastroenterol.* 2005; 11:705–7. [PubMed: 15655826]
63. Zhao L, Liu Y, Sun X, He M, Ding Y. Overexpression of T lymphoma invasion and metastasis 1 predict renal cell carcinoma metastasis and overall patient survival. *J Cancer Res Clin Oncol.* 2010

64. Li Y, et al. UTRN on chromosome 6q24 is mutated in multiple tumors. *Oncogene*. 2007; 26:6220–8. [PubMed: 17384672]
65. Nelson WJ. Remodeling epithelial cell organization: transitions between front-rear and apical-basal polarity. *Cold Spring Harb Perspect Biol*. 2009; 1:a000513. [PubMed: 20066074]
66. Lambert JM, et al. Tiam1 mediates Ras activation of Rac by a PI(3)K-independent mechanism. *Nat Cell Biol*. 2002; 4:621–5. [PubMed: 12134164]

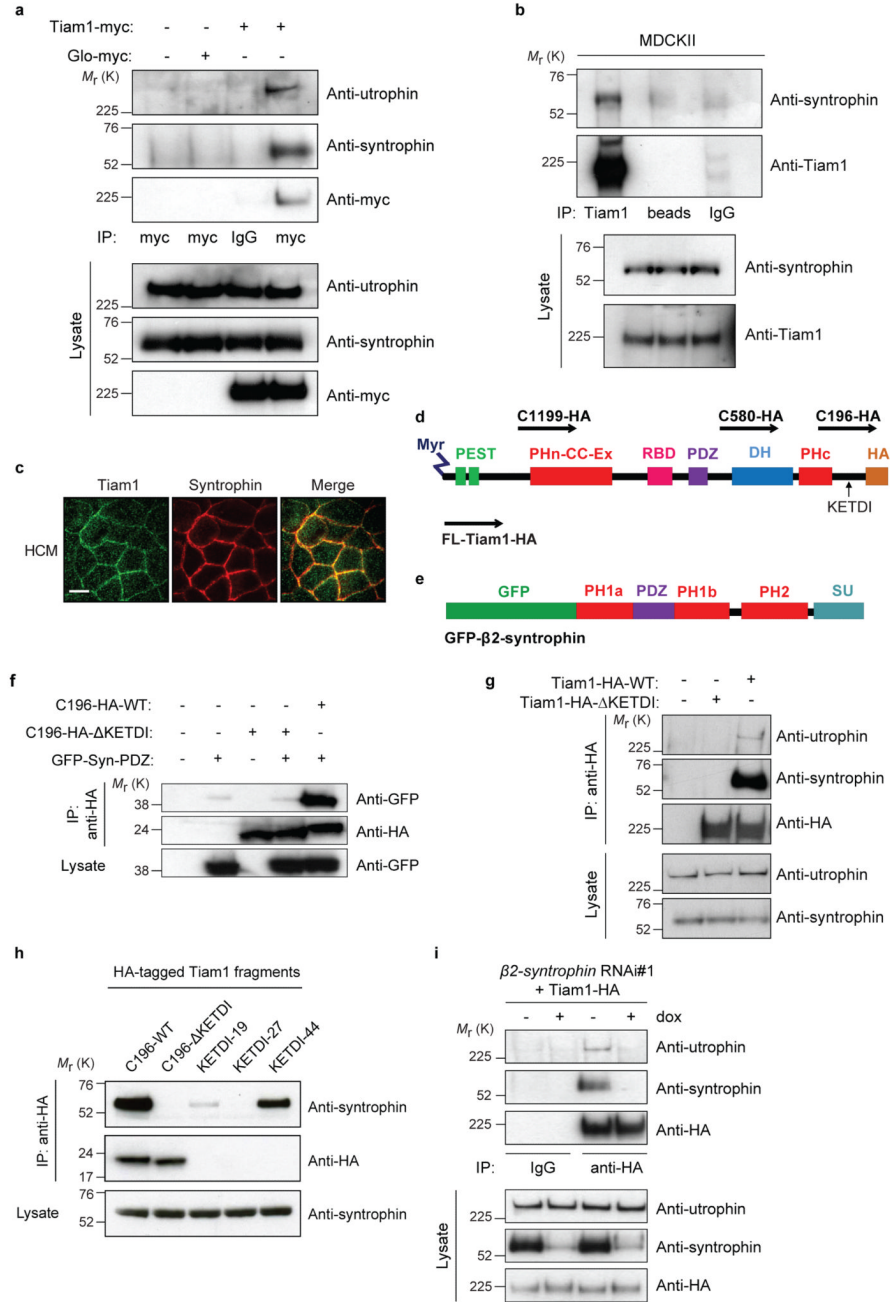


Figure 1. Tiam1 interacts with the β2-syntrophin PDZ domain using an internal PDZ-binding motif. (a) Exogenous Tiam1-myc expressed in HEK293T cells was immunoprecipitated with anti-myc antibody. Co-precipitated endogenous syntrophin and endogenous utrophin were detected by immunoblotting. (b) Endogenous Tiam1 from MDCKII cells was immunoprecipitated with anti-Tiam1 antibody and co-precipitated endogenous syntrophin was detected by immunoblotting. (c) MDCKII cells cultured in high calcium medium (HCM) were fixed and stained by immunofluorescence for Tiam1 and syntrophin. Scale bar represents 10 μm. (d) Schematic representation of the domain structure of full-length (FL) HA-tagged Tiam1 (FL-Tiam1-HA). Horizontal arrows indicate the various N-terminally

truncated Tiam1-HA constructs used. Vertical arrow indicates where the internal KETDI PDZ binding motif (PBM) is approximately located. Myr, myristoylation site; PEST, motif rich in Proline (P), Glutamic acid (E), Serine (S), and Threonine (T); PHn-CC-EX, N-terminal pleckstrin homology, coiled-coil, extended structure; RBD, Ras binding domain; PDZ, PSD-95/Dlg1/ZO-1; DH, Dbl homology; PHc, C-terminal pleckstrin homology; HA, hemagglutinin tag. (e) Schematic representation of the domain structure of GFP- β 2-syntrophin. GFP, green fluorescent protein tag; SU, Syntrophin Unique domain; PH1a and PH1b, split pleckstrin homology domain; PH2, second pleckstrin homology domain. (f) Tiam1-C196-HA-WT and Tiam1-C196-HA- Δ KETDI were transfected into HEK293T cells with the GFP-tagged PDZ domain of β 2-syntrophin (GFP-Syn-PDZ). The exogenous Tiam1 fragments were immunoprecipitated with anti-HA antibody and co-precipitated GFP-Syn-PDZ was detected by immunoblotting. (g) Tiam1-HA-WT or Tiam1-HA- Δ KETDI were expressed in HEK293T cells and immunoprecipitated with anti-HA antibody. Co-precipitated endogenous syntrophin and utrophin were detected by immunoblotting. (h) The indicated HA-tagged Tiam1 fragment constructs were expressed in HEK293T cells and immunoprecipitated with anti-HA antibody. Co-precipitated endogenous syntrophin was detected by immunoblotting with anti-syntrophin antibody. (i) Tiam1-HA was immunoprecipitated from MDCKII cells which were also engineered to express shRNA targeting β 2-syntrophin (β 2-syntrophin RNAi#1) following addition of doxycycline (+ dox). Co-precipitated endogenous syntrophin and utrophin were detected by immunoblotting. All data shown are representative of at least three independent experiments. IP, indicates immunoprecipitation. Uncropped images of blots are shown in Supplementary Information, Fig. S9.

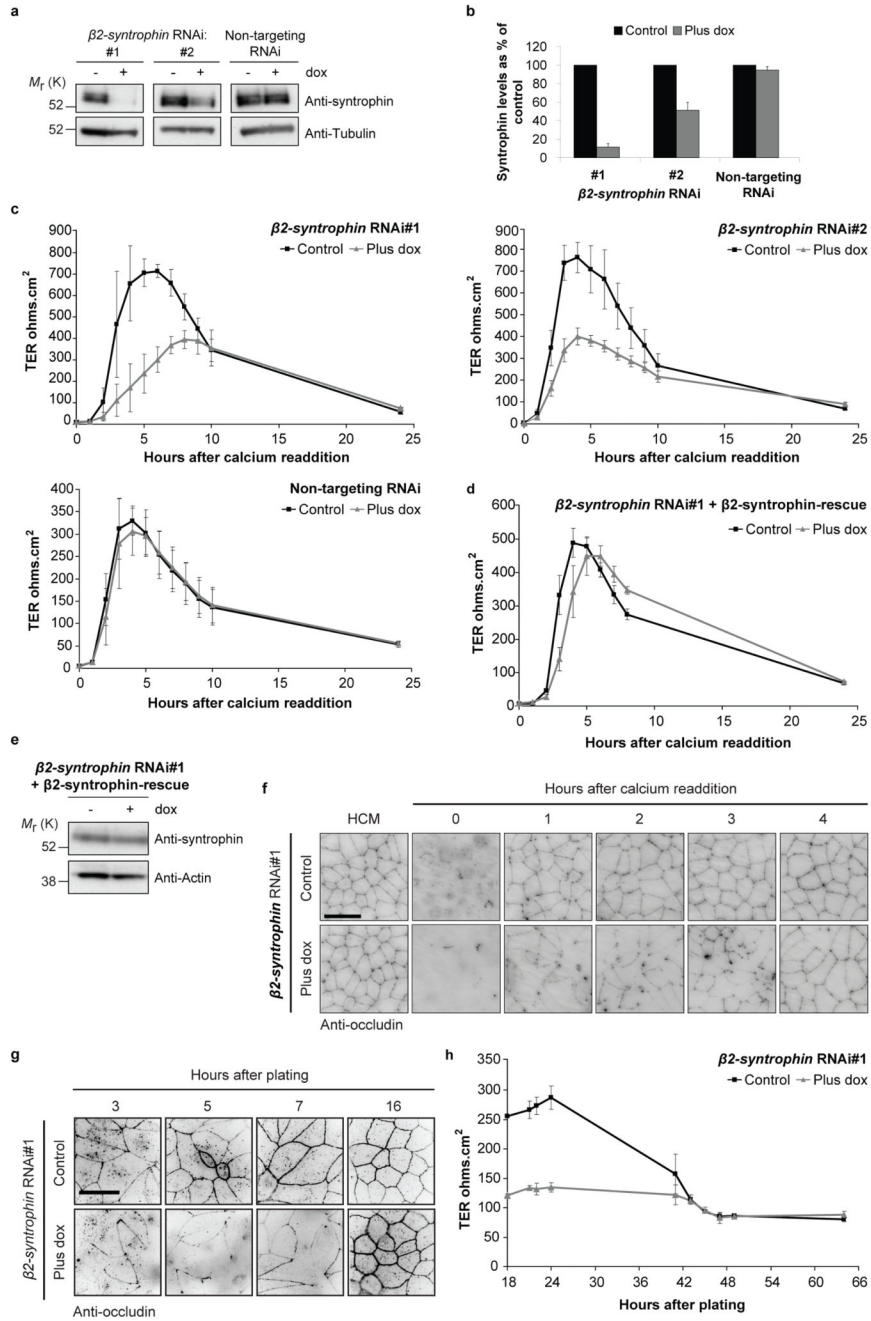


Figure 2. $\beta 2$ -syntrophin regulates TJ assembly in MDCKII cells. (a) MDCKII cells with doxycycline-inducible expression of one of two separate shRNAs targeting $\beta 2$ -syntrophin ($\beta 2$ -syntrophin RNAi#1, #2) or a non-targeting control shRNA (Non-targeting RNAi) were treated with (+) or without (-) doxycycline (dox) where indicated. Levels of syntrophin and Tubulin were detected by immunoblotting. A representative immunoblot is shown. (b) Graph quantifying $\beta 2$ -syntrophin knockdown, n=3. (c) Calcium switch (CS) TER readings from $\beta 2$ -syntrophin RNAi#1, #2 or Non-targeting RNAi MDCKII cells treated with (Plus dox) or without (Control) dox, n=3. (d) CS TER readings from $\beta 2$ -syntrophin RNAi#1 MDCKII cells expressing shRNA-resistant $\beta 2$ -syntrophin ($\beta 2$ -syntrophin-rescue) treated with (Plus dox) or

without (Control) dox, n=3. (e) Immunoblot showing syntrophin levels in *β2-syntrophin* RNAi#1 cells expressing *β2-syntrophin-rescue* treated with (+) or without (-) dox. Actin is used as a loading control. (f) *β2-syntrophin* RNAi#1 MDCKII cells treated with (Plus dox) or without (Control) dox were fixed from high calcium medium (HCM), or at the indicated CS time-points, and stained by immunofluorescence for occludin. Panels show representative images from one of three independent experiments. (g) *β2-syntrophin* RNAi#1 MDCKII cells treated with (Plus dox) or without (Control) dox were fixed at the indicated time-points after plating and stained by immunofluorescence for occludin. Panels show representative images from one of three independent experiments. (h) TER readings from *β2-syntrophin* RNAi#1 MDCKII cells treated with (Plus dox) or without (Control) dox at the indicated time-points after plating, n=3. n represents number of independent experiments. Results in b, c, d and h represent mean values±s.e.m for the indicated number of independent experiments. Scale bars represent 30 μm. Uncropped images of blots are shown in Supplementary Information, Fig. S9.

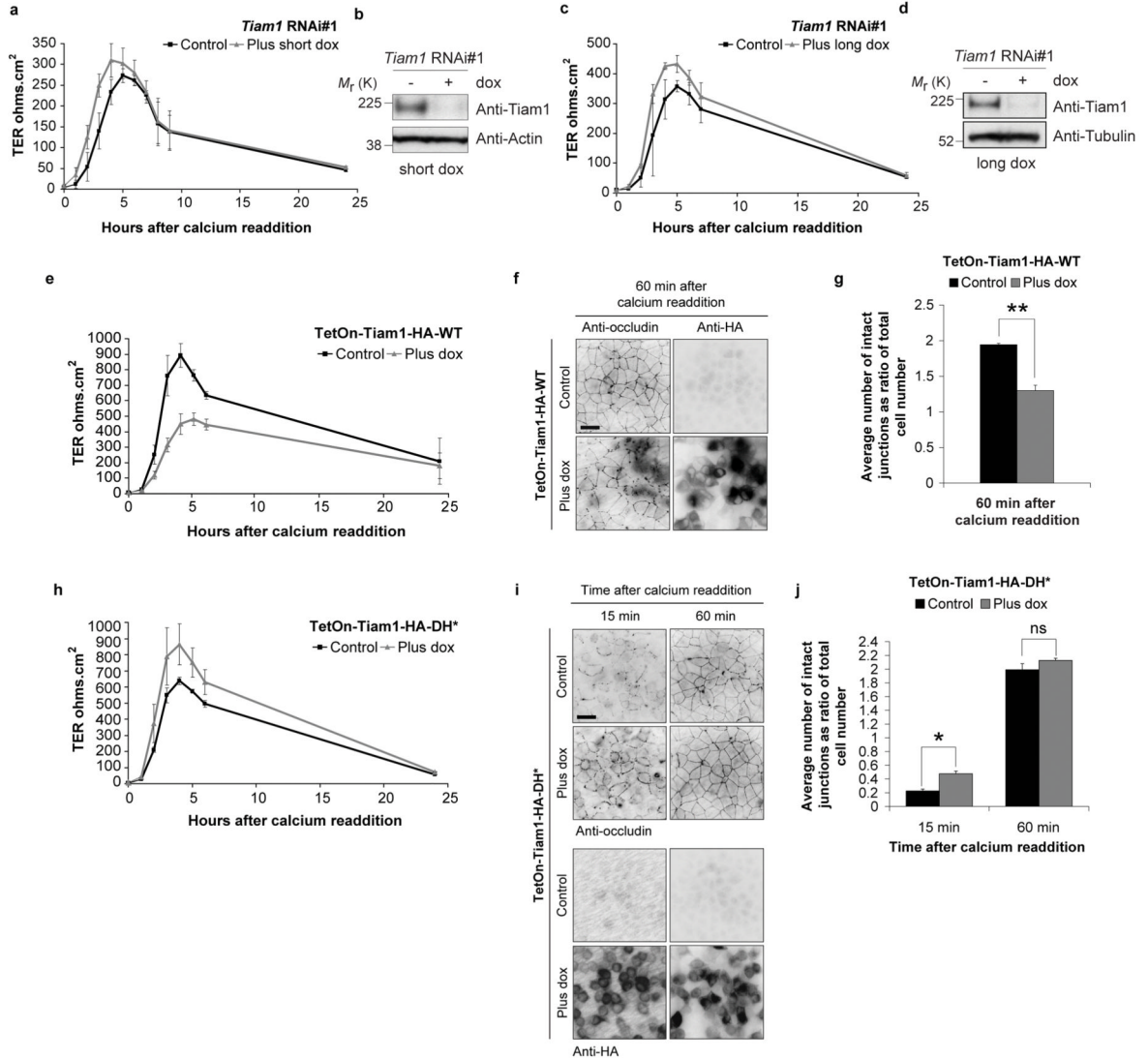


Figure 3. Tiam1-induced Rac activity impedes TJ assembly in MDCKII cells. (a) CS TER readings for MDCKII cells inducibly expressing a *Tiam1* shRNA (*Tiam1* RNAi#1) treated with (Plus dox) or without (Control) dox for 7 days (short dox), n=3. (b) Representative immunoblot showing the extent of Tiam1 knockdown for cells in (a). Actin was used as a loading control. (c) As for (a) but cells treated with (Plus dox) or without (Control) dox for 3 weeks (long dox), n=3. (d) Representative immunoblot showing the extent of Tiam1 knockdown for cells in (c). Tubulin was used as a loading control. (e) CS TER readings for MDCKII cells inducibly over-expressing Tiam1-HA-WT (TetOn-Tiam1-HA-WT) treated with (Plus dox) or without (Control) dox, n=3. (f) Representative images of TetOn-Tiam1-HA-WT MDCKII cells treated with (Plus dox) or without (Control) dox fixed 60 min after CS and stained by immunofluorescence for occludin and HA. (g) Graph showing average number of intact junctions as a ratio of total cell number, n=4. t-test: ** P<0.005. (h) CS TER readings for MDCKII cells inducibly over-expressing Tiam1-HA-DH* (TetOn-Tiam1-HA-DH*) treated with (Plus dox) or without (Control) dox, n=4. (i) Representative images of TetOn-Tiam1-HA-DH* MDCKII cells treated with (Plus dox) or without (Control) dox fixed 15

and 60 min after CS and stained by immunofluorescence for occludin and HA. (j) Graph showing average number of intact junctions as a ratio of total cell number, $n=3$. t-test: 15 min * $P<0.05$, 60 min $P=0.310$ (ns). n represents number of independent experiments. ns indicates no significant difference. Results in a, c, e, g, h and j represent mean values \pm s.e.m for the indicated number of independent experiments. Scale bars represent 30 μ m. Uncropped images of blots are shown in Supplementary Information, Fig. S9.

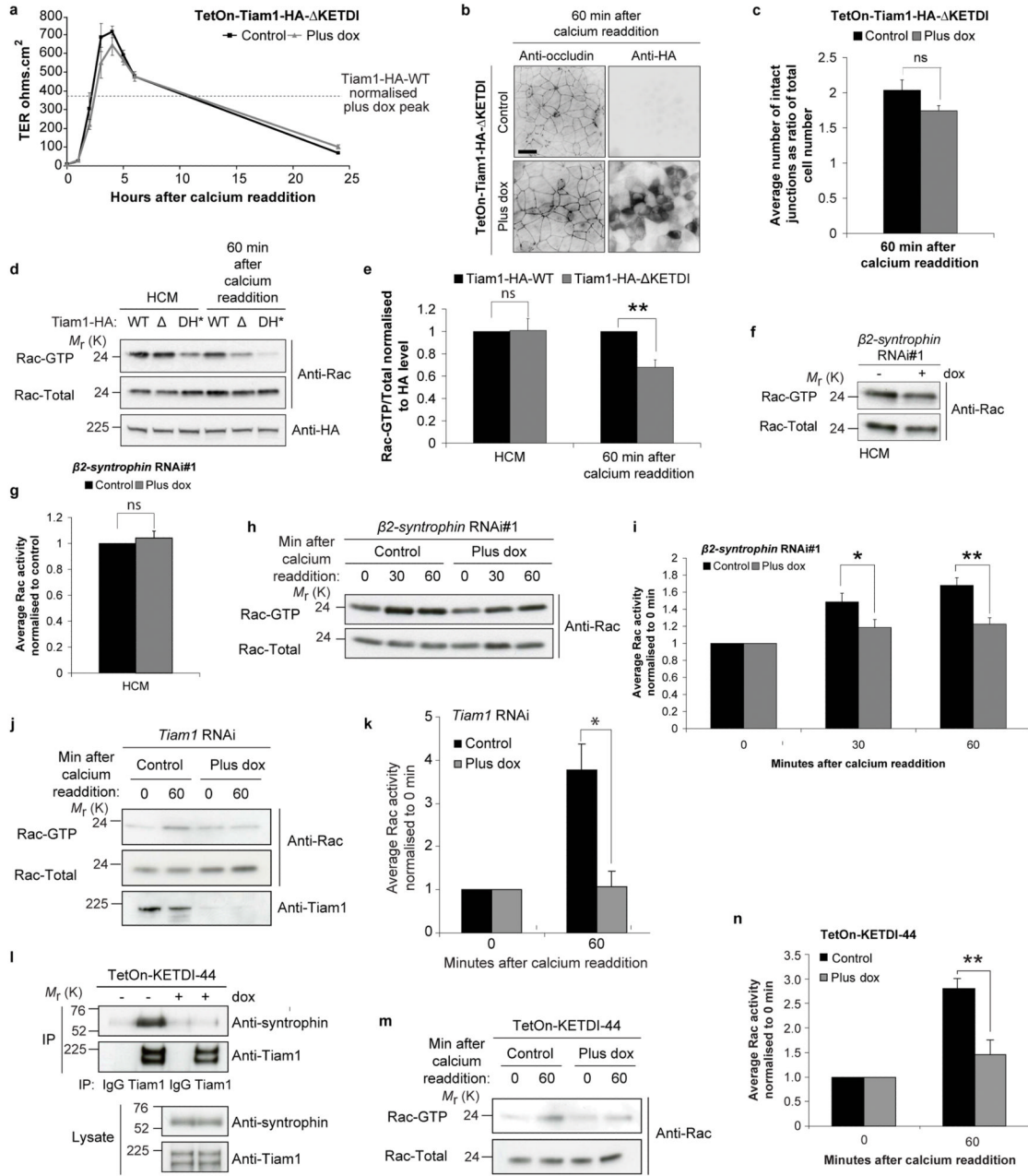


Figure 4.

β 2-syntrophin promotes Tiam1-Rac activity during TJ assembly. (a-c) MDCKII cells inducibly over-expressing Tiam1-HA- Δ KETDI (TetOn-Tiam1-HA- Δ KETDI) were treated with (Plus dox) or without (Control) dox. (a) Calcium switch (CS) TER readings, n=3. The dotted line represents the TER peak from dox-treated TetOn-Tiam1-HA-WT cells normalised to that of control TetOn-Tiam1-HA- Δ KETDI cells. (b) Representative images of cells fixed 60 min after CS and stained by immunofluorescence for occludin and HA. (c) Graph showing average number of intact junctions as a ratio of total cell number, n=3. t-test: P=0.223 (ns). (d) Dox-treated confluent TetOn-Tiam1-HA-WT, TetOn-Tiam1-HA- Δ KETDI and TetOn-Tiam1-HA-DH* cells were maintained in high calcium medium (HCM) or

subjected to 60 min CS and subsequently lysed and assayed for Rac activity. (e) Quantification of (d), n=5. t-test: HCM P=0.938 (ns), 60 min switch ** P<0.005. (f-i) Confluent $\beta 2$ -*syntrophin* RNAi#1 cells were treated with (+ or plus dox) or without (- or control) dox. (f) Immunoblot from cells maintained in HCM and subsequently lysed and assayed for Rac activity. (g) Quantification of (f), n=3. Paired t-test: P=0.381 (ns). (h) Immunoblot from cells subjected to 0, 30 or 60 min CS and subsequently lysed and assayed for Rac activity. (i) Quantification of (h), n=5. Paired t-test: 30 min * P<0.05, 60 min ** P<0.005. (j) Immunoblot from confluent *Tiam1* RNAi cells treated with (Plus dox) or without (Control) dox, subjected to 0 or 60 min CS and subsequently lysed and assayed for Rac activity. (k) Quantification of (j), n=3. t-test: * P<0.05. (l-n) TetOn-KETDI-44 cells were treated with (+) or without (-) dox. (l) Endogenous Tiam1 was immunoprecipitated with anti-Tiam1 antibody and co-precipitated endogenous syntrophin was detected by immunoblotting with anti-syntrophin antibody. (m) Immunoblot from cells subjected to 0 or 60 min CS and subsequently lysed and assayed for Rac activity. (n) Quantification of (m), n=3. t-test: 60 min ** P<0.005. n represents number of independent experiments. ns indicates no significant difference. Results in a, c, e, g, i, k and n represent mean values \pm s.e.m for the indicated number of independent experiments. Scale bars represent 30 μ m. Uncropped images of blots are shown in Supplementary Information, Fig. S9.

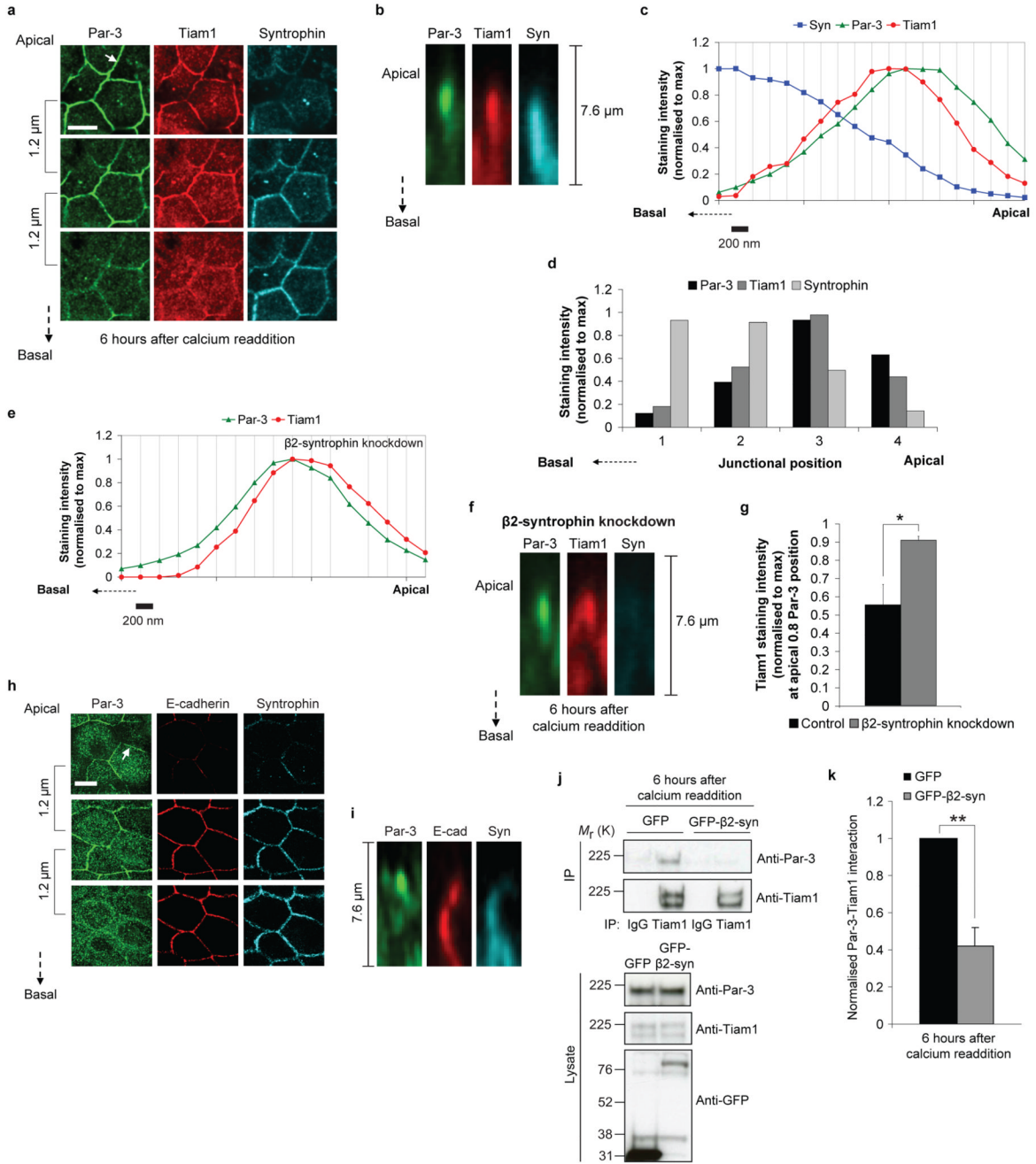
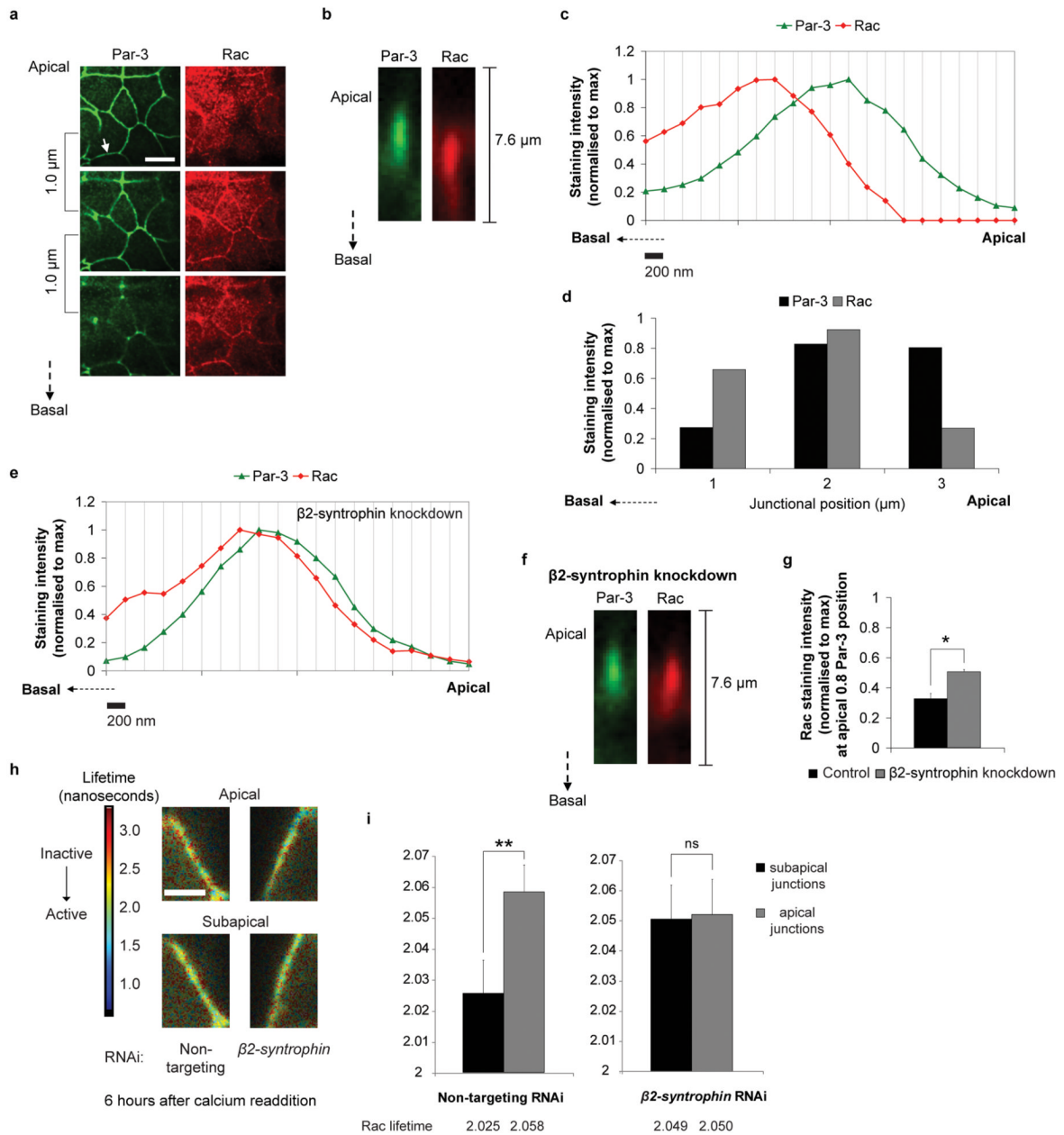


Figure 5.

β 2-syntrophin, Par-3 and Tiam1 localise differently along the apicobasal junctional axis. (a-g) β 2-syntrophin RNAi#1 MDCKII cells treated with (β 2-syntrophin knockdown) or without (Control) dox were subjected to 6 hours calcium switch (CS) and then fixed and stained with anti-Par-3, anti-Tiam1 and anti-syntrophin antibodies. (a) Representative images of Control cells in the x/y planes at three different z-steps with 1.2 μ m separation. (b) Images of Par-3, Tiam1 and Syntrophin stainings in the x/z plane at a cross-section along the junction highlighted in (a) by a white arrow. (c) Quantification of Par-3, Tiam1 and Syntrophin staining intensities (normalised to their own maximal intensity) at the junction shown in (b). (d) A representative experiment quantifying average staining intensities for

Par-3, Tiam1 and Syntrophin (normalised to their own maximal intensity) from individual junctions of control cells at four junctional positions (1 μm apart on the z-axis). (e) Quantification of Par-3 and Tiam1 staining intensities (normalised to their own maximal intensity) at a representative junction from a β 2-syntrophin knockdown cell. (f) Images of Par-3, Tiam1 and Syntrophin stainings in the x/z plane at a cross-section along the junction quantified in (e). (g) Quantification of Tiam1 staining intensities at apical junction positions (where Par-3 staining intensity was closest to 0.8) of individual junctions in control and β 2-syntrophin knockdown cells, n=3. t-test: * $P < 0.05$. (h) MDCKII cells fixed and stained with anti-Par-3, anti-E-cadherin and anti-syntrophin antibodies 6 hours after CS. Representative images are shown in the x/y planes at three different z-steps with 1.2 μm separation. (i) Images of the x/z plane at a cross-section along the junction highlighted in (h) by a white arrow. (j) Endogenous Tiam1 was immunoprecipitated from GFP-alone or GFP- β 2-syntrophin over-expressing MDCKII cells 6 hours after CS with anti-Tiam1 antibody and co-precipitated endogenous Par-3 was detected by immunoblotting with anti-Par-3 antibody. (k) Quantification of (j), n=3, t-test: ** $P < 0.005$. n represents number of independent experiments. Results in g and k represent mean values \pm s.e.m for the indicated number of independent experiments. Scale bars represent 10 μm . Syn, Syntrophin. Uncropped images of blots are shown in Supplementary Information, Fig. S9.

**Figure 6.**

An apicobasal Rac activity gradient at cell-cell junctions. (a-g) β 2-syntrophin RNAi#1 MDCKII cells treated with (β 2-syntrophin knockdown) or without (Control) dox subjected to 3 hours calcium switch (CS), were fixed and stained with anti-Par-3 and anti-Rac antibodies. (a) Representative images of Control cells in the x/y planes at three different z-steps with 1.0 μm separation. (b) Images of Par-3 and Rac stainings in the x/z plane at a cross-section along the junction highlighted in (a) by a white arrow. (c) Quantification of Par-3 and Rac staining intensities (normalised to their own maximal intensity) at the junction shown in (b). (d) A representative experiment quantifying average staining intensities for Par-3 and Rac (normalised to their own maximal intensity) from individual junctions of control cells at three junctional positions (1 μm apart on the z-axis). (e) Quantification of Par-3 and Rac staining intensities (normalised to their own maximal intensity) at the junction shown in (b) for β 2-syntrophin knockdown cells. (f) Images of Par-3 and Rac stainings in the x/z plane at a cross-section along the junction highlighted in (a) by a white arrow for β 2-syntrophin knockdown cells. (g) Quantification of Rac staining intensity (normalised to their own maximal intensity) at the apical 0.8 μm Par-3 position for β 2-syntrophin knockdown cells. (h) Lifetime (nanoseconds) of Rac activity at apical and subapical junctions for non-targeting and β 2-syntrophin RNAi cells 6 hours after calcium readdition. (i) Rac lifetime at subapical and apical junctions for non-targeting and β 2-syntrophin RNAi cells.

Quantification of Par-3 and Rac staining intensities (normalised to their own maximal intensity) at a representative junction from a β 2-syntrophin knockdown cell. (f) Images of Par-3 and Rac stainings in the x/z plane at a cross-section along the junction quantified in (e). (g) Quantification of Rac staining intensities at apical junction positions (where Par-3 staining intensity was closest to 0.8) of individual junctions in control and β 2-syntrophin knockdown cells, n=3. Paired t-test: * P<0.05. (h, i) FLIM-FRET analysis of Non-targeting or β 2-syntrophin RNAi Raichu-Rac MDCKII cells 6 hours after CS. (h) Representative lifetime images in the x/y plane at apical and subapical junctional positions. Fluorescence lifetimes of GFP are shown in false colours. Red indicates high lifetime (inactive), yellow/green indicates low lifetime (active). (i) Average fluorescence lifetimes found at subapical and apical junctional positions, n=3. Paired t-test: Non-targeting RNAi ** P<0.005, β 2-syntrophin RNAi P=0.094 (ns). n represents number of independent experiments. ns indicates no significant difference. Results in g and i represent mean values \pm s.e.m. for the indicated number of independent experiments. Scale bars represent 10 μ m.

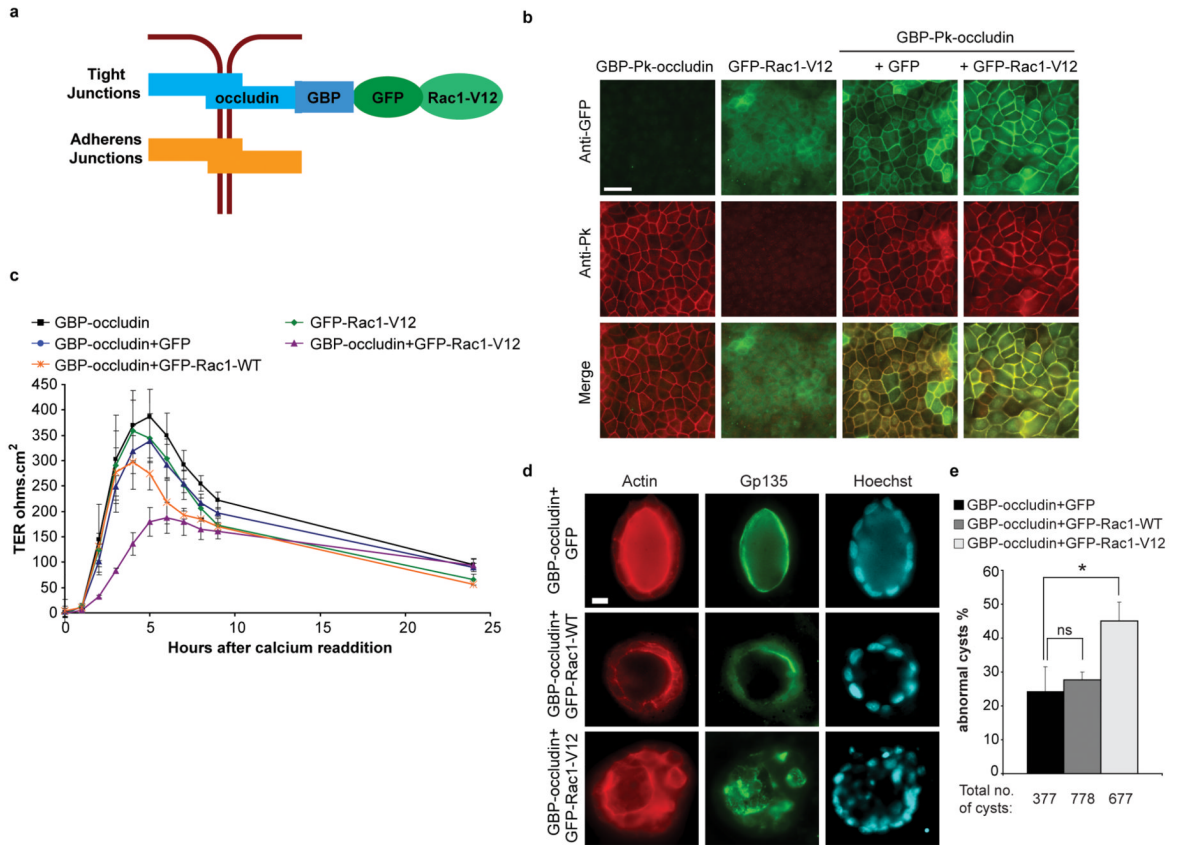
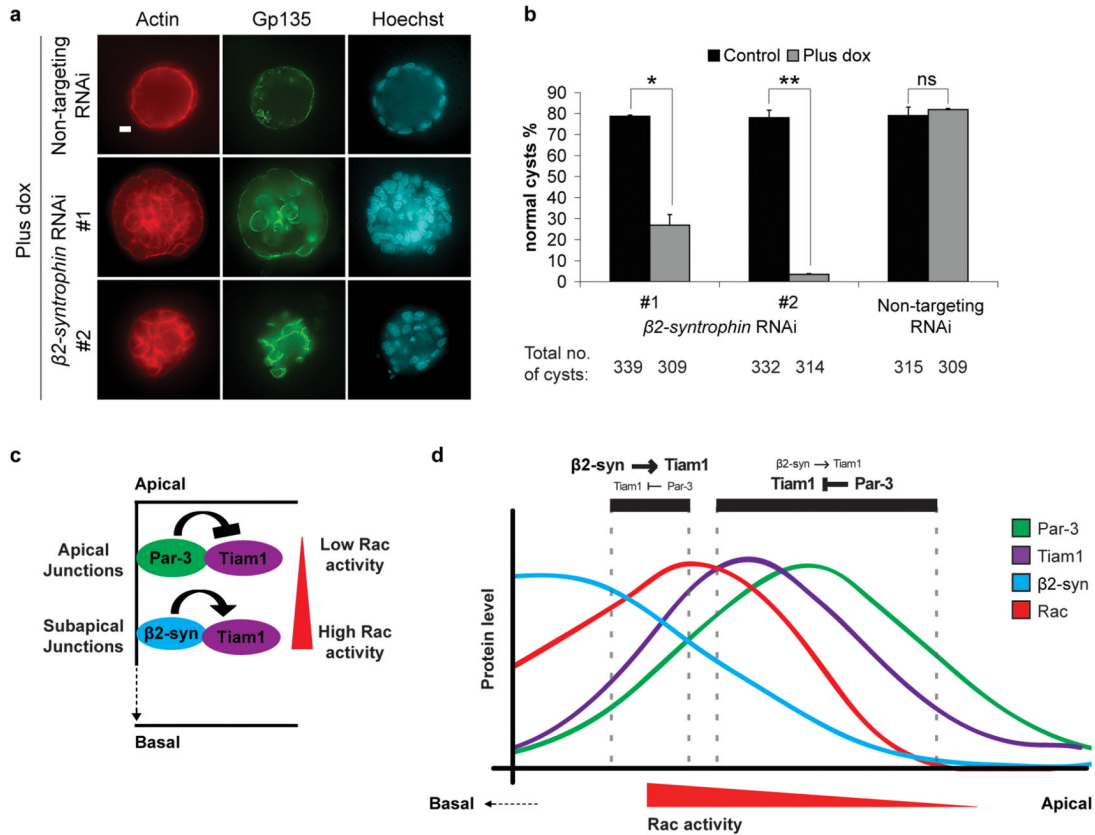


Figure 7.

The cell-cell junction Rac activity gradient promotes TJ assembly and apicobasal polarity. (a) Schematic representation of the GBP-GFP system used to target GFP-tagged proteins to TJs. GBP, GFP binding protein. (b-e) MDCKII cell lines expressing either GBP-Pk-occludin, GFP-Rac1-V12, GBP-Pk-occludin and GFP, GBP-Pk-occludin and GFP-Rac1-V12 or GBP-Pk-occludin and GFP-Rac1-WT, were generated. (b) Representative images of cell lines indicated, fixed and stained with anti-GFP and anti-Pk antibodies. The images shown are from a single z-section. Scale bar represents 30 μ m. (c) CS TER readings: GBP-occludin (n=4), GFP-Rac1-V12 (n=6), GBP-occludin+GFP (n=9), GBP-occludin+GFP-Rac1-V12 (n=7) and GBP-occludin+GFP-Rac1-WT (n=3). (d) Images showing single cross-sections of representative cysts of GBP-occludin+GFP, GBP-occludin+GFP-Rac1-V12 or GBP-occludin+GFP-Rac1-WT expressing MDCKII cells grown in collagen I matrix and stained for Actin (red, left panel), Gp135 (green, middle panel) as an apical marker, and Hoechst (blue, right panel) to show nuclei. Scale bar represents 10 μ m. (e) Quantification of abnormal cysts from (d), n=3. The total number of cysts analysed for each cell line is shown. Paired t-test: GFP control vs. Rac1-WT P=0.572 (ns), GFP control vs. Rac1-V12 * P<0.05. n represents number of independent experiments. ns indicates no significant difference. Results in c and e represent mean values \pm s.e.m for the indicated number of independent experiments.

**Figure 8.**

$\beta 2$ -syntrophin promotes apicobasal polarity. (a) Images show single cross-sections of representative cysts of $\beta 2$ -syntrophin RNAi#1, #2, or Non-targeting RNAi MDCKII cells treated with dox and stained for Actin (red, left panel), Gp135 (green, middle panel), and Hoechst (blue, right panel). (b) Quantification of (a) and Supplementary Information, Fig. S8a, n=3. The total number of cysts analysed is shown. Paired t-test: $\beta 2$ -syntrophin RNAi#1 * P<0.05, $\beta 2$ -syntrophin RNAi#2 ** P<0.005, Non-targeting RNAi P=0.600 (ns). (c) Model depicting the differential localisations of Par-3 and $\beta 2$ -syntrophin and their differential effects on Tiam1-Rac activity at cell-cell junctions. (d) Model depicting the differential but overlapping localisations of $\beta 2$ -syntrophin, Par-3, Tiam1 and Rac at cell-cell junctions, which enable them to promote an apicobasal junctional Rac activity gradient. $\beta 2$ -syn, $\beta 2$ -syntrophin. n represents number of independent experiments. Results in b represent mean values \pm s.e.m for the indicated number of independent experiments. Scale bar represents 10 μ m.